



Widespread elevated concentrations of gaseous elemental mercury in Guanajuato, Mexico, centuries after historical silver refining by mercury amalgamation



Ainsleigh Loria^a, Yann Rene Ramos-Arroyo^b, Diana Rocha^c, Gustavo Cruz-Jiménez^c, Israel Razo-Soto^d, Ma. Catalina Alfaro de la Torre^e, Debbie Armstrong^a, Saúl Guerrero^f, Feiyue Wang^{a,*}

^a Centre for Earth Observation Science, and Department of Environment and Geography, University of Manitoba, Winnipeg, Manitoba R3T 2N2, Canada

^b Departamento de Ingeniería Geomática y Hidráulica, Universidad de Guanajuato, Guanajuato, Guanajuato C.P. 36000, Mexico

^c Departamento de Farmacia, Universidad de Guanajuato, Guanajuato, Guanajuato C.P. 36050, Mexico

^d Facultad de Ingeniería, Universidad Autónoma de San Luis Potosí, San Luis Potosí, San Luis Potosí C.P. 78290, Mexico

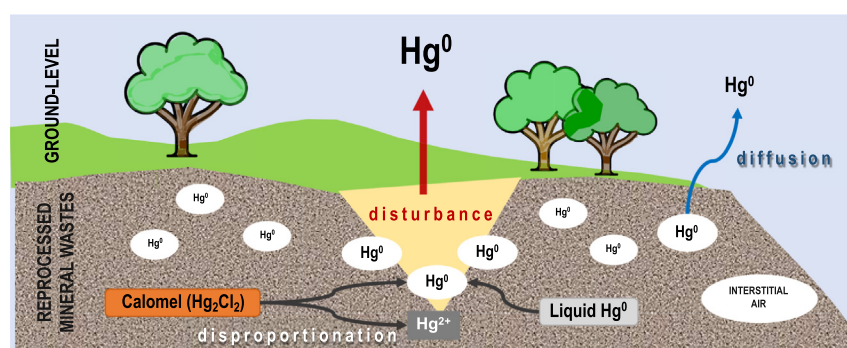
^e Facultad de Ciencias Químicas, Universidad Autónoma de San Luis Potosí, San Luis Potosí, San Luis Potosí C.P. 78210, Mexico

^f School of Culture, History and Language, Australian National University, Canberra, ACT, 0200, Australia

HIGHLIGHTS

- Mining in the 16th to 19th centuries constituted a large source of atmospheric mercury.
- Mercury emissions persists from historical silver refining in Hispanic America.
- In Guanajuato, Mexico, some legacy mercury is present as calomel.
- Disproportionation of calomel contributes to gaseous mercury concentrations.
- This provides a continuous source of legacy mercury emissions.

GRAPHICAL ABSTRACT



ARTICLE INFO

Editor: Mae Sexauer Gustin

Keywords:

Mercury pollution
Historical silver mining
Patio process
Calomel
Hispanic America
Minamata convention

ABSTRACT

Silver (Ag) production in Hispanic America between the 16th and 19th centuries is thought to be one of the largest sources of anthropogenic mercury (Hg) emissions in history. Recent reviews of the chemistry behind the patio process, which used Hg amalgamation to extract Ag from ore, reveal that a large amount of the Hg may not have been immediately released to the atmosphere; instead, it may have been captured in the form of calomel (Hg_2Cl_2 , in which Hg exists as monovalent Hg^I) and remained in the local environment. Here we show that Hg used in the patio process centuries ago in the Guanajuato Mining District of Mexico continues to elevate present-day concentrations of gaseous elemental mercury (GEM) throughout the region. In the ground-level air, GEM ranged from 8 to 454 ng m^{-3} , exceeding the Northern Hemispheric average ($\sim 1.4 \text{ ng m}^{-3}$) by up to two orders of magnitude. Much higher concentrations, up to $44,700 \text{ ng m}^{-3}$, were found in the interstitial air of reprocessed mineral wastes, sediment, and soil. These highly elevated present-day GEM values are due, at least in part, to the disproportionation of legacy calomel, as supported by the presence of Hg^I in the reprocessed wastes and by the GEM release pattern from calomel disproportionation. Our results imply that the contribution of historical Ag refining to atmospheric Hg emissions must be re-evaluated to account for calomel and its subsequent disproportionation and releases of GEM to the present-day.

* Corresponding author.

E-mail address: feiyue.wang@umanitoba.ca (F. Wang).

<http://dx.doi.org/10.1016/j.scitotenv.2022.157093>

Received 21 April 2022; Received in revised form 26 June 2022; Accepted 27 June 2022

Available online 30 June 2022

0048-9697/© 2022 The Authors. Published by Elsevier B.V. This is an open access article under the CC BY-NC-ND license (<http://creativecommons.org/licenses/by-nc-nd/4.0/>).

1. Introduction

Mercury (Hg) is a global contaminant that is emitted into the atmosphere by natural and anthropogenic sources, such as volcanic activities, coal combustion, and silver (Ag) and gold (Au) refining processes that employ Hg amalgamation (AMAP/UNEP, 2019). To protect human health and the environment from the adverse effects of Hg, a global treaty, the Minamata Convention, entered into force in 2017 with the goal of reduction of anthropogenic Hg emissions (AMAP/UNEP, 2019). One of the major challenges in evaluating the effectiveness of the Minamata Convention is the uncertainty associated with Hg released from anthropogenic activities, especially those from historical activities such as Hg-aided Ag refining (known as the patio process) that took place on a large scale in Hispanic America from the late 16th to the end of the 19th century (Outridge et al., 2018). Whereas some estimates (Amos et al., 2013; Nriagu, 1993; Streets et al., 2011; Streets et al., 2017) placed Ag refining in Hispanic America as one of the largest anthropogenic Hg sources in history, other studies hinted its contribution might be much smaller (Guerrero, 2012; Guerrero, 2016; Guerrero, 2018; Outridge et al., 2018; Streets et al., 2019; Zhang et al., 2014).

Nriagu (1993) was the first to recognize the global significance of Hg emissions from Ag refining in Hispanic America, estimating a total of 2.0×10^5 t of Hg being released to the atmosphere from 1570 to 1900, which would have accounted for ~13 % of the global total anthropogenic Hg releases throughout human history (Streets et al., 2017). This and subsequent studies (Camargo, 2002; Hagan et al., 2011; Nriagu, 1993; Nriagu, 1994; Robins et al., 2012) based their estimates on the assumption that the Hg emissions from Ag mining in Hispanic America were similar to those generated in artisanal Au mining, where 60–85 % of the Hg was emitted to the atmosphere and only a minor fraction was lost to local land and water bodies. Even with a conservative emission factor between 40 and 52 %, global Hg budget models show that Ag refining in Hispanic America would have contributed substantially to the present-day, global atmospheric and oceanic Hg concentrations and inventories (Amos et al., 2013; Streets et al., 2011; Streets et al., 2017).

However, by reviewing the chemistry behind the patio process employed in historical Ag refining in Hispanic America, Guerrero (2012, 2016, 2018) brought attention to the fact that the amalgamation processes involved in Ag and Au extraction were fundamentally different. Gold is typically present in ore in its elemental form that can be directly extracted by amalgamation with elemental Hg (Hg^0). The amalgam would be heated to recover the Au with Hg^0 being released as a vapor, some of which would be recovered and reused in future refining cycles, and the rest lost to the atmosphere. In contrast, most of the Ag in deep ore deposits in the Americas occurs as monovalent Ag^1 (acanthite (Ag_2S) and chlorargyrite ($AgCl$)) (Guerrero, 2016; Sillitoe, 2009) that needs to be reduced to Ag^0 before amalgamation could take place. In the patio process, liquid Hg^0 was employed to serve both purposes. Silver ore, salt and water were first blended into a slurry in an outdoor courtyard (“patio”), to which liquid Hg^0 was added and mixed for several days by continuous treading with horses, mules, or people (Guerrero, 2016; Johnson and Whittle, 1999). In this process, Ag^1 was first reduced by Hg^0 into Ag^0 to enable the amalgamation process; the redox reaction simultaneously produced calomel (Hg_2Cl_2 , in which Hg exists as monovalent Hg^1) as a by-product (Johnson and Whittle, 1999). Based on the chemistry involved, Guerrero (2012, 2016) calculated that as much as 66–93 % of the Hg used in Ag extraction by the patio process was transformed into calomel, with no more than 7–34 % lost as Hg^0 to the soil, waterways, and atmosphere. Measurements carried out in the 19th century in Mexican and American Ag refining centers suggested that only up to 3 % of Hg was emitted directly to the atmosphere during operations (Guerrero, 2018). Guerrero (2018) estimated that the rest was lost to local land and water bodies in the form of calomel (84 %) or liquid Hg^0 (13 %).

Applying Guerrero’s low atmospheric Hg emission factor for Ag refining, more recent global Hg modeling revealed that the contribution of Ag mining in Hispanic America to the global atmospheric and oceanic Hg

levels and inventories would be much lower than previously thought (Outridge et al., 2018; Streets et al., 2019; Zhang et al., 2014). This would be in better agreement with historical atmospheric Hg deposition data derived from sediment core records from remote lakes and Hg measurements in the deep ocean, both of which indicate only modest Hg emissions from mining activities during the pre-industrial era (Engstrom et al., 2014; Outridge et al., 2018). However, the presence of calomel in historical Ag mining regions has not been studied.

As part of an international collaborative effort to understand local and global implications of the fate of legacy Hg, here we test the hypothesis that at least some of the Hg used in the patio process centuries ago in Hispanic America remains in the local environment as calomel and continues to emit Hg to the air to the present-day.

2. Materials and methods

2.1. Study area

The Guanajuato Mining District (GMD) (Fig. 1), Mexico, was recognized as one of the most lucrative Ag-producing regions in the world during the Spanish Colonial era, producing more than 8000 t of Ag for the period from 1654 to 1805 alone (Guerrero, 2017). The patio process was used until the 19th century when it was gradually replaced by cyanidation and by flotation since 1946 (Ramos-Arroyo et al., 2004). More details of the GMD and regional information are provided in the Supporting Information (SI; Text S1 and Fig. S1).

Twenty-six sites in GMD were studied in July 2019 (Fig. 1, Table S1), 22 of which are located within the City of Guanajuato, a narrow valley that hosts the renowned Ag mines that were exploited throughout the Colonial Era. The study sites include reprocessed mineral wastes, sediment/soil, and other sites that may be historically significant to the amalgamation process (e.g., former *haciendas*, mine areas). Many of the sites are frequented daily by residents and tourists alike, whereas others are more secluded.

The distinction between “reprocessed mineral waste sites” and “sediment/soil sites” was based on the texture of the substrate and their origin. The reprocessed mineral waste sites contain fine materials originated from former amalgamation wastes from *haciendas* that have since been reprocessed by either cyanidation or flotation to obtain residual amounts of Ag. Some mineral wastes have been discarded on mountain tops on the outskirts of the city (e.g., La Perlita), while others have been deposited in residential areas (e.g., Cerro del Cuarto). Sediment/soil sites are typically associated with water bodies (e.g., rivers, dams, reservoirs). The sites along the river in the urban area (e.g., Río Guanajuato, Río Pastita and Plaza Ranas) are in proximity of former *haciendas*, which are known to have spanned the riverside. *Haciendas* housed the amalgamation process and from there the Hg-containing wastes would be discarded into the river. Hydrological sites outside the urban area (e.g., Puenteillas and La Purísima) are located downstream at the end of the regional basin approximately 20 km south of the city (Fig. S1). Sites categorized as “others” were unlikely to contain mineral wastes from the patio process in the present day. Examples of sites in the others category include parks in the vicinity of old mines, former *haciendas* that have been re-purposed (e.g., parking structures, hotels), and constituents of the famous underground traffic tunnels of Guanajuato which runs the original course of the Guanajuato River. More details about each site and potential human exposure risks are given in Table S2.

2.2. Measurement of GEM

In-situ, real-time concentrations of GEM in the ground-level air and interstitial air were measured by Zeeman atomic absorption spectroscopy on a Lumex RA-915M Hg analyzer (Lumex Instruments, Mission, Canada) (Sholupov et al., 2004). Measurements were taken in the data logger mode to cross-check with the field notes, at a resolution of every second to capture any rapid changes in the GEM concentration. The detection limit was 1.0 ng m^{-3} and the working GEM range was up to $20,000 \text{ ng m}^{-3}$

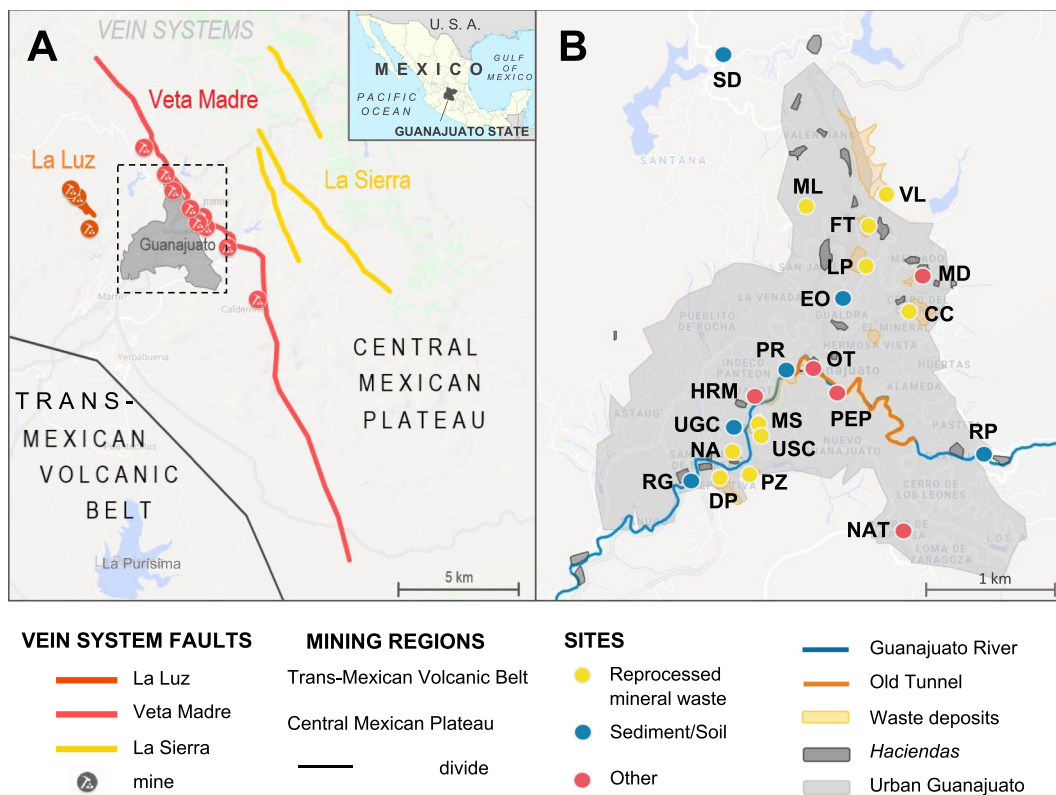


Fig. 1. Maps showing A) the silver-bearing veins in the Guanajuato Mining District, Mexico, and B) an enlarged view of the dashed rectangle area of A) showing the study sites in and near the city of Guanajuato (shaded in gray). Details of the study sites are shown in Tables S1 and S2. Base maps were modified from Google Maps and Google Earth.

(Lumex Instruments). Quality assurance and quality control (QA/QC) was done by daily verification of the deviation value ($\pm 20\%$ with the stated manufacturer range) and by running a zero check every 15 min.

Two types of measurements were made: Surveys and Profiles. At Survey sites, GEM was measured for 5–120 min in the ground-level air only,

including the ambient air (at approximately 100 cm above the ground surface), at the ground surface (both undisturbed and when disturbed by gently kicking over the topsoil), in crevasses, and near walls and other features of structures that may be associated with the historical amalgamation process (e.g., Fig. 2A). At Profile sites, in addition to the ground-level air

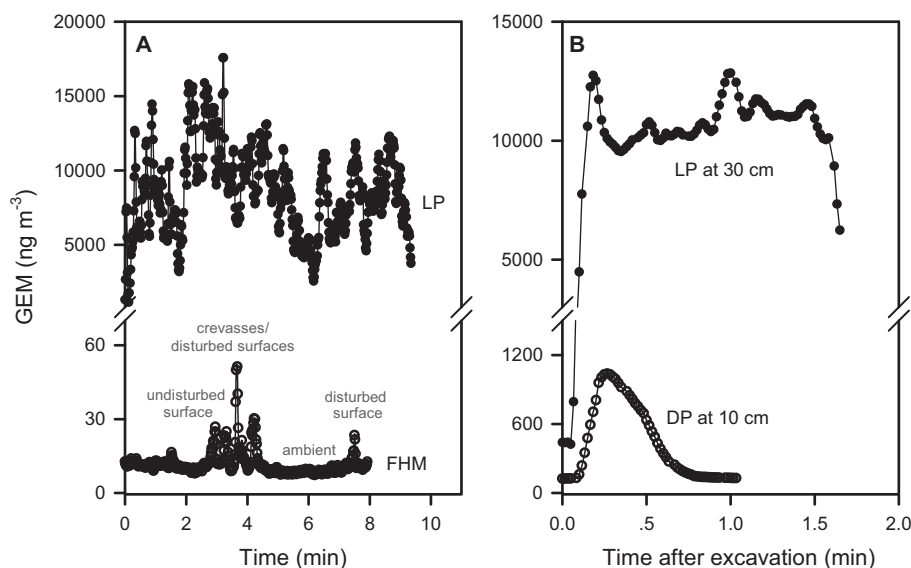


Fig. 2. Examples of time series patterns of gaseous elemental mercury (GEM) concentrations in A) the ground-level air at a Survey site, FHM (former hacienda Mellado, a present-day tourist look-out site on the grounds of the preserved ruins of a former hacienda) as the surface went through various disturbances, and at a Profile site, LP (La Perlita, a mountain site where reprocessed mineral wastes were discarded), upon surface disturbance on a hot, sunny day; B) the interstitial air at site LP at a depth of 30 cm and at another Profile site, DP (Deportiva, near a present-day sports complex containing discarded reprocessed mineral wastes) at 10 cm.

measurement, GEM was also measured in the interstitial air of reprocessed mineral wastes, and sediment/soil. Successive depth excavations, typically in increments of 5 cm, were made from the ground surface downwards, reaching a maximum depth of up to 150 cm, as permitted by the substrate. The excavations were done using a Dutch auger and were followed immediately by a GEM measurement at the given depth. The GEM value typically increased to a maximum within a minute, and thereafter decreased due to dilution by the ambient air introduced by the excavation and measurement (e.g., Fig. 2B). A measurement was considered complete once the signal stabilized, and the maximum value at each excavated depth was recorded as the GEM concentration in the interstitial air at that depth.

2.3. Measurement of total Hg and monovalent Hg in reprocessed mineral wastes, soil, and sediment

Reprocessed mineral waste, soil and sediment samples were collected on the same day of the GEM measurements for the analysis of total Hg (Hg_T) concentration and to evaluate the potential for occurrence of Hg^I . The samples were collected into Whirl-pak bags and shipped in coolers to the University of Manitoba.

A total of 42 samples were analyzed for Hg_T by atomic absorption spectroscopy on a direct Hg analyzer (Hydra-II_c, Teledyne Leeman Labs) following U.S. EPA Method 7473 (U.S. EPA, 2007). The samples were analyzed without freeze-drying and Hg_T concentrations were not corrected for water content. Between 1 and 50 mg of sample were weighed into a quartz boat using a microbalance (MS104S, Mettler Toledo). Calibration and QA/QC were done with certified reference materials including MESS-4 (marine sediment, $Hg_T = 90 \pm 40 \text{ ng g}^{-1}$ (average \pm standard deviation) and PACS-3 (marine sediment, $Hg_T = 2980 \pm 360 \text{ ng g}^{-1}$) from the National Research Council of Canada, and NIST 2709A (San Joaquin soil, $Hg_T = 900 \pm 200 \text{ ng g}^{-1}$) from the National Institute of Standards and Technology of the U.S.

Twenty-nine of the freeze-dried samples were further analyzed for Hg^I following a qualitative method involving 2-mercaptoethanol (2-ME) extraction (Wang et al., 2020). Briefly, the freeze-dried samples were extracted with a 0.2 % (v/v) 2-ME solution for 2 h on a mechanical shaker at 200 rpm at room temperature, and filtered with 0.2 μm polyethersulfone filters (Puradisc 25, Whatman). Separation of Hg^I from divalent Hg^{II} in the filtrates was achieved on an ion chromatograph (IC) (ICS 5000+, Dionex) with a C_{18} column (Agilent InfinityLab Poroshell 120 EC- C_{18}) and a 0.5 % 2-ME mobile phase, which was interfaced with an inductively coupled plasma-mass spectrometer (ICP-MS; Agilent 8900 triple quadrupole) for Hg detection. Samples of a commercially available calomel solid (see below) were extracted and analyzed following the same procedure. More details are provided in the SI (Text S2).

2.4. Calomel disproportionation experiment

A laboratory experiment was carried out to examine the GEM release pattern from calomel disproportionation in the presence of UV-visible light. Approximately 0.1 g of calomel (99 % pure, Alfa Aesar) was weighed into a glass beaker. The beaker was inserted into the chamber of a SunTest XLS+ solar simulator (Atlas, Mount Prospect, USA) for an hour ($\lambda = 300\text{--}800 \text{ nm}$, irradiance = 700 W m^{-2}). GEM produced from calomel disproportionation was measured by placing the inlet tubing of the Lumex Hg analyzer near the outflow grid of the solar simulator, following the same QA/QC procedures as described above. Prior to the experiment, GEM was also measured in the laboratory ambient air away from the solar simulator, near the outflow of the solar simulator, and inside the solar simulator chamber to allow for comparisons.

2.5. Data analysis

GEM concentrations in the ground-level air were reported as arithmetic means of the ambient air, disturbed and undisturbed surface measurements when the data followed a normal distribution, and as medians otherwise.

GEM concentrations in the interstitial air were reported as the maximum values at specific depths. Medians and ranges of GEM were also reported for each site category and across the entire study area as the data did not follow a normal distribution. Statistical analyses were done using SigmaPlot v13 (SysStat Software Inc.). The ANOVA on ranks and the Mann-Whitney Rank Sum analyses were conducted at a significance level of 0.05.

3. Results

3.1. GEM in the ground-level air

At Survey sites, GEM values in the ground-level air were generally stable, but increased upon disturbance of the surface or during measurements in crevasses of walls (Fig. 2A). At Profile sites, the ground-level air measurement was comprised of the mean of the stabilized ambient air measurement and stabilized surface measurements (Fig. 2A).

Across the entire study area in Guanajuato, the median GEM concentration in the ground-level air was 28 ng m^{-3} , ranging from 7 ng m^{-3} at the New Access Tunnel (NAT) to 454 ng m^{-3} at Cerro del Cuarto (CC) (Fig. 4, Table S2). Among site categories, the median GEM values in the ground-level air were generally lower at the sediment/soil (21 ng m^{-3}) and other (23 ng m^{-3}) sites than at the reprocessed mineral waste sites (56 ng m^{-3}), although the differences between the groups were not statistically significant (ANOVA on ranks, $p = 0.11$). Spatially, the ground-level air GEM concentrations were generally higher in urban areas (range: 7 to 454 ng m^{-3}) than those in rural areas (range: 8 to 200 ng m^{-3}), such as Puentecillas (PC) and La Purísima (PP).

3.2. GEM in the interstitial air

At most of the Profile sites, the GEM concentration in the interstitial air increased rapidly following the excavation of the reprocessed mineral wastes, sediment or soil material, and then decreased within seconds (e.g., Site DP in Fig. 2B). The only exception was the La Perlita (LP) reprocessed waste site where elevated GEM concentrations at each depth were sustained for more than one minute before decreasing (Fig. 2B). At the same site, a sustained, elevated GEM signal (consistently between 2000 and $18,000 \text{ ng m}^{-3}$ over 10 min) was also observed at the disturbed surface of the wastes (Fig. 2A).

With two exceptions (sites FT and CC), GEM concentrations in the interstitial air at all other Profile sites were higher than at the surface or in the ambient air (Fig. 3, Table S2). No apparent trend was found between depth and GEM concentrations in the interstitial air of wastes, sediment and soil, as the depth where the interstitial GEM concentration peaked varied greatly from 10 cm at DP to 270 cm at PC. The maximum GEM values in the interstitial air varied between 95 ng m^{-3} at Santana Creek (SC) and $44,700 \text{ ng m}^{-3}$ at Plaza Ranas (PR), with a median value of 865 ng m^{-3} (Fig. 4B). The maximum GEM of $44,700 \text{ ng m}^{-3}$ was observed downtown at Plaza Ranas near a former *hacienda* along the old path of the Guanajuato River that has since been paved into a road. Note that this maximum concentration exceeded the upper limit of the working range ($20,000 \text{ ng m}^{-3}$) of the Lumex Hg analyzer, so it is possible that actual concentrations could be higher.

The site category with the highest median GEM concentration in the interstitial air was the reprocessed waste sites (1090 ng m^{-3}), followed by the sediment/soil sites (251 ng m^{-3}), though the differences between the mean values were not statistically significant (Mann-Whitney Rank Sum Test, $p = 0.198$). Interstitial air GEM was not measured at Survey sites. The spatial distribution of maximum GEM concentrations observed in the interstitial air of reprocessed mineral wastes, sediment, and soil are illustrated in Fig. S2.

3.3. Hg_T and Hg^I in reprocessed wastes, soil, and sediment

The Hg_T concentrations in the 42 waste, sediment, and soil samples varied over five orders of magnitude, ranging from $0.068 \mu\text{g g}^{-1}$ at

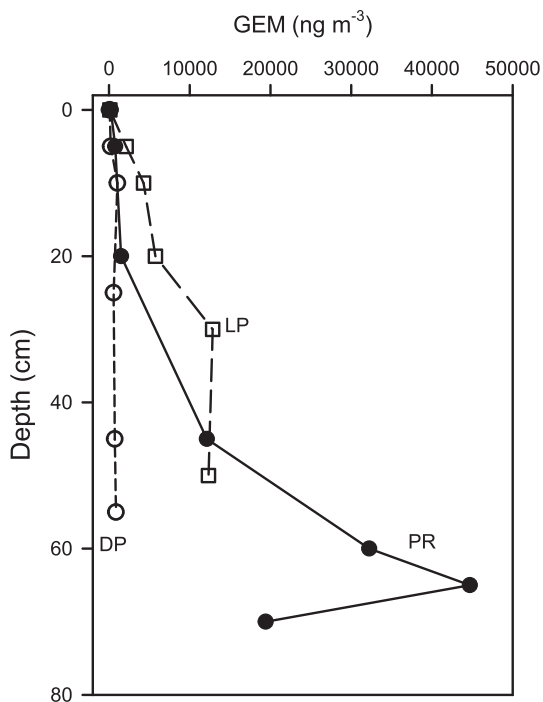


Fig. 3. Examples of vertical distribution patterns of maximum gaseous elemental mercury (GEM) concentrations at three Profile sites DP (Deportiva), LP (La Perlita), and PR (Plaza Ranas, near a former hacienda along the old path of the Guanajuato River).

Puentecillas to 622 $\mu\text{g g}^{-1}$ at the Pastita River (Table S3), with a median value of 7.04 $\mu\text{g g}^{-1}$. The Hg_T concentrations were higher in urban areas (median: 14.7 $\mu\text{g g}^{-1}$, range: 0.177 to 620 $\mu\text{g g}^{-1}$) than rural areas (median: 7.04 $\mu\text{g g}^{-1}$, range: 0.068 to 10.6 $\mu\text{g g}^{-1}$). These values are in good agreement with Hg concentrations found in present-day soil near historical Ag mining sites in Potosí of Bolivia (up to 155 $\mu\text{g g}^{-1}$) (Hagan et al., 2011; Higuera et al., 2012), and in the vicinity of former haciendas in Cedral of Mexico (up to 116 $\mu\text{g g}^{-1}$ in soil and 548 $\mu\text{g g}^{-1}$ in amalgamation wastes) (Leura Vicencio et al., 2017; Morton-Bermea et al., 2015).

The 2-ME extraction method showed the presence Hg^I (and Hg^{II}) in all the 29 samples analyzed (Table S3). Examples of resulting IC-ICP-MS chromatograms are shown in Fig. 5, which clearly indicates the presence of both Hg^I and Hg^{II} in the extracted soil sample from Plaza Ranas (PR), as their respective peaks were well separated with retention times matching those of the Hg^I and Hg^{II} standards.

3.4. Calomel disproportionation experiment

Results from the calomel disproportionation experiment are shown in Fig. 6. GEM measurements taken in the laboratory and outside of the solar simulator prior to the experiment are indicative of background concentrations of the laboratory and showed little variation (Fig. 6A, B), with mean values of 2.9 and 2.8 ng m^{-3} , respectively. The mean GEM value measured inside the solar simulator chamber prior to the photodegradation experiment was 6 ng m^{-3} (Fig. 6C). As soon as the calomel sample was placed inside the solar simulator and the light was activated, the GEM signal rose rapidly and peaked at 102 ng m^{-3} within minutes (Fig. 6D). GEM then decreased slowly over the next 30 min before plateauing at a sustained and elevated concentration of 50 ng m^{-3} for the remainder of the one-hour experiment.

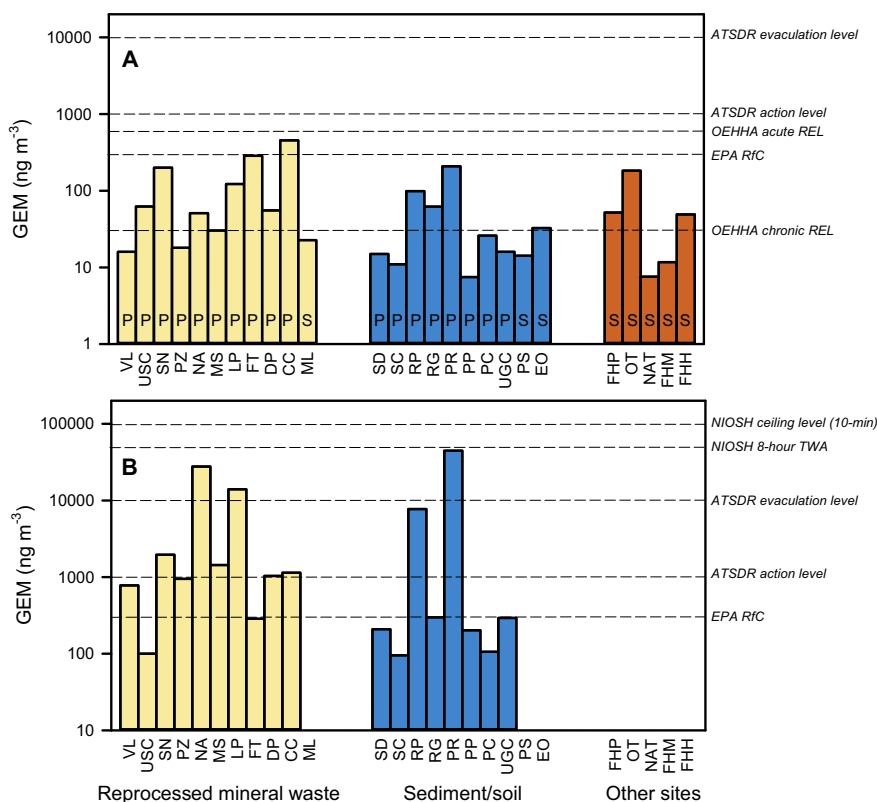


Fig. 4. Summary of gaseous elemental mercury (GEM) concentrations in and around the city of Guanajuato, Mexico. A) Mean or median GEM concentrations in the ground-level air. B) Maximum GEM concentrations in the interstitial air. Bars labelled with a “P” refer to Profile sites, and those with an “S” refer to the Survey site data. Dashed lines indicate various air quality guidelines for GEM. ATSDR: U.S. Agency for Toxic Substances and Disease Registry; EPA: U.S. Environmental Protection Agency; NIOSH: U.S. National Institute for Occupational Safety and Health; OEHHA: California Office of Environmental Health Hazard Assessment.

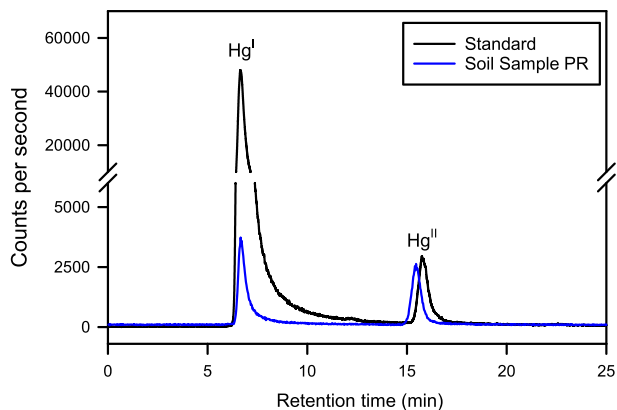


Fig. 5. Ion chromatography-inductively coupled plasma-mass spectrometry (IC-ICP-MS) chromatograms of ^{202}Hg from a mixed Hg^{I} ($100 \mu\text{g L}^{-1}$) and Hg^{II} ($10 \mu\text{g L}^{-1}$) standard solution (black line) and the 2-mercaptoethanol extract of the Plaza Ranas (PR) soil sample (blue line), showing the presence of Hg^{I} (and Hg^{II}) in the soil sample.

4. Discussion

4.1. Widespread incidences of highly elevated GEM values across the GMD

As shown in Fig. 4 and Table S2, GEM concentrations in the ground-level ambient air throughout the study area consistently exceeded the global average in the Northern Hemisphere (1.3 to 1.5 ng m^{-3}) (AMAP/UNEP, 2019), often by one to two orders of magnitude, in public, residential, and secluded spaces. Much higher GEM concentrations were found in the interstitial air at the reprocessed mineral waste and sediment/soil sites within the urban area of Guanajuato (Fig. S2). The maximum GEM value of $44,700 \text{ ng m}^{-3}$ was observed at Plaza Ranas near a former hacienda, which is over an order of magnitude higher than that reported beneath the topsoil of a former patio site at the Cerro Rico mine in Potosí, Bolivia (3000 ng m^{-3}) (Higueras et al., 2012).

4.2. Source and processes causing the elevated air Hg concentrations

Based on the geology and mineralogy of the ores in the GMD, there are no significant natural sources of Hg in this region, with Hg concentrations in the epithermal veins reportedly less than $1 \mu\text{g g}^{-1}$ (Randall-Roberts

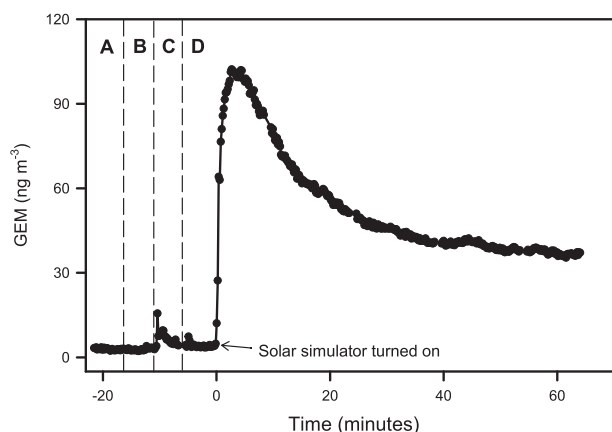
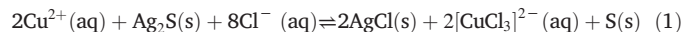


Fig. 6. Release of gaseous elemental mercury (GEM) from calomel disproportionation inside a solar simulator, showing GEM concentrations of A) the ambient laboratory air prior to the start of the experiment, B) near the outflow of the solar simulator prior to the start of the experiment, C) the chamber of the solar simulator prior to the start of the experiment, and D) near the outflow of the solar simulator during the experiment. Time zero denotes when the solar simulator was turned on.

et al., 1994). The widespread, present-day high concentrations of GEM in the ground-level ambient air and interstitial air are thus attributed to the legacy Hg used in historical Ag refining.

Based on the work of Johnson and Whittle (1999), Guerrero (2018) and the results from this study, the chemical reactions involved in the patio process can be summarized in Fig. 7. $\text{Ag}_2\text{S}(\text{s})$ in the ore was first converted to $\text{AgCl}(\text{s})$ in the presence of Cu^{2+} and Cl^- in aqueous solution:



Hg^0 was then added, reducing $\text{AgCl}(\text{s})$ to Ag^0 , while itself being oxidized to calomel:



Subsequently, the amalgam was formed from the reaction of Ag^0 with excess Hg^0 .



The amalgam was then heated to recover Ag. Some of the Hg^0 was recycled, with the rest rapidly lost to the air, or as residual liquid Hg^0 to the soil, refining wastes, and waterways where it may eventually be volatilized to the air (Lacerda and Salomons, 1999).

In contrast to Guerrero's hypothesis that the calomel would function as a permanent chemical sink for most of the Hg used in Ag refining (Guerrero, 2017), results from this study indicated that the calomel in the local environment has been slowly degrading and generating GEM over time. As a Hg^{I} compound, calomel is known to be susceptible to a disproportionation reaction, in which oxidation and reduction occur simultaneously, producing Hg^0 (GEM) and Hg^{II} (Schlüter, 2000):



The HgCl_2 formed initially during the disproportionation reaction would be readily converted to the more stable $\text{HgS}_{(\text{s})}$, especially in alkaline, reducing, or anaerobic conditions (Barnett et al., 1997; Svensson et al., 2006), which can occur during long-term burial of mineral wastes in organic-rich soil and sediment (Barnett et al., 1997; Kim et al., 2004). The dominance of $\text{HgS}_{(\text{s})}$ has been confirmed in soil and tailings from the patio process in Cedral, Mexico (Bayer, 2013; Morton-Bermea et al., 2015), and in Potosí, Bolivia (Hagan et al., 2011).

It is possible that a fraction of the calomel could have disproportionated during the patio process, which we refer to as “instantaneous emissions”. The patios were open-air chemical reactors, where the amalgamation slurry was mixed by the feet of workers and hooves of animals for several weeks (Guerrero, 2017), and exposed to the elements such as sunlight that could have induced calomel disproportionation. A large amount of calomel, however, would have been discarded into the river with the rest of the refining wastes, and/or buried in soil and sediment, where it would slowly degrade and form GEM through disproportionation. We refer any GEM emitted after the patio process (e.g., GEM formed through calomel disproportionation) as “cumulative emissions”.

In the waste piles, the GEM formed during calomel disproportionation and from elemental Hg^0 would be initially confined to the interstitial air within the wastes. The maximum or the peak GEM concentration measured in this study likely reflects a cumulation of the disproportionated calomel and residual elemental Hg^0 from the patio process confined in the interstitial air of the wastes. The cumulated GEM can be slowly emitted to the ambient air via diffusion or more rapidly upon physical disturbance to the matrix (e.g., Fig. 2), with the latter resulting in acute GEM exposure events. In both cases, the subsequent emissions of GEM are regarded as cumulative emissions that contribute to the elevated ground-level GEM concentrations observed present-day. Estimating the mass budget of calomel over the past several hundred years would require a better knowledge of the factors that may affect the rate of the calomel disproportionation reaction including

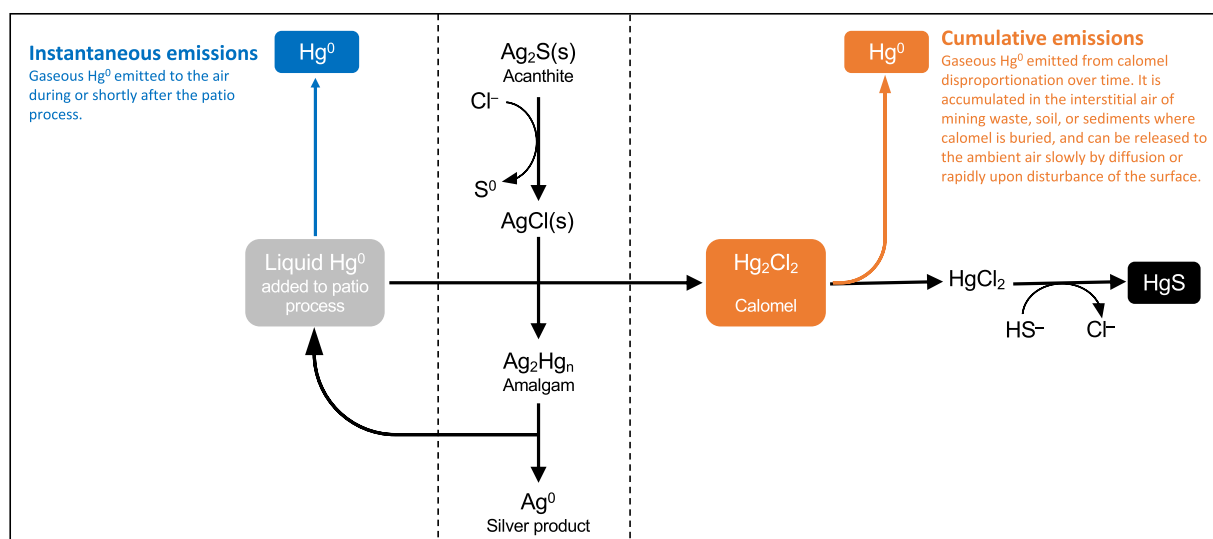


Fig. 7. An updated scheme, based on Johnson and Whittle (1999), Guerrero (2018) and this work, of major chemical reactions involved in the patio process of historical silver (Ag) refining in Hispanic America. The central dashed box highlights reactions involving Ag. Some of the liquid mercury added to the patio process was emitted to the air in the form of elemental mercury (Hg^0) during or shortly after the process (“instantaneous emissions”, shown in the left panel), whereas the rest was converted to calomel (Hg_2Cl_2) and remained in the local environment, continuing to release Hg^0 (and Hg^{II}) to the present-day via disproportionation (“cumulative emissions”, shown in the right panel).

temperature, precipitation, pore space, aeration, exposure to sunlight, presence of certain elements, and the effects of reprocessing of the wastes.

4.3. Further support for the role of calomel

Standard mineralogical analytical techniques, including X-ray diffraction, scanning and transmission electron microscopy, were unable to identify calomel in the soil/mineral waste samples, as those techniques required much higher Hg concentrations. Instead, the presence of calomel is supported by two independent and indirect lines of evidence. First, the occurrence of calomel in the sediment and soil containing mineral wastes is supported by the Hg^{I} peak in all the waste, soil, and sediment samples analyzed by the 2-ME method (Fig. 6, Table S2). We chose the 2-ME method, because other Hg speciation techniques for solid matrices such as thermos-desorption atomic spectroscopy are not capable of identifying Hg^{I} due to peak overlaps (Wang et al., 2020). Although the 2-ME method is not quantitative (Wang et al., 2020), the chromatograms explicitly revealed the presence of Hg^{I} in the samples (Fig. 6, Table S2). While the chemical structures and stabilities of possible Hg^{I} compounds in the environment remain poorly studied, calomel is the most probable Hg^{I} compound in the Guanajuato samples given the chemical reactions involved in the patio process (Fig. 7).

The second line of evidence is the calomel disproportionation experiment. Both the in-situ GEM measurements at La Perlita (Fig. 2A) and the GEM pattern from the laboratory calomel disproportionation experiment (Fig. 6) exhibit a consistent and elevated GEM signal that is sustained beyond the ambient baseline for an extended period of time. The La Perlita measurements were conducted at the top of a mountain on a hot and sunny day where the freshly exposed surface of the wastes was subjected to sunlight, i.e., conditions that are conducive to calomel disproportionation. The GEM pattern measured can be readily explained by calomel disproportionation under a solar simulator (Fig. 6).

It should be noted that our work does not rule out the role of other Hg species in the emission of GEM. Any legacy liquid Hg^0 from the original patio process, if preserved in mining wastes, soil, or sediment to this day (although no liquid Hg^0 was visually identified in any of our study sites or samples), would be susceptible to volatilization to become GEM. Photo-enhanced GEM emissions have also been reported in synthesized or natural soil substrates containing Hg^0 or Hg^{II} (e.g., HgS , HgCl_2 , corderoite ($\text{Hg}_3\text{S}_2\text{Cl}_2$)) (Gustin et al., 2002).

4.4. Human exposure implications

To put the GEM concentrations into context, ground-level GEM concentrations at 14 of the 26 study sites surpass the California Office of Environmental Health Hazard Assessment (OEHHA) chronic reference exposure level (REL) (30 ng m^{-3}), while one site exceeds the U.S. Environmental Protection Agency (EPA) reference concentration of 300 ng m^{-3} (Fig. 4). These ground-level air GEM measurements are concentrations that the public are readily and possibly chronically exposed to, as they represent ambient air measurements from above-ground surveys and upon surface disturbance of the mineral wastes, soil, or sediment.

The maximum interstitial air GEM values surpassed the U.S. Agency for Toxic Substances and Disease Registry (ATSDR) evacuation level ($10,000 \text{ ng m}^{-3}$) at three sites, including Noria Alta (NA), La Perlita (LP) and Plaza Ranas (PR). The maximum GEM value of $44,700 \text{ ng m}^{-3}$ at Plaza Ranas approaches the U.S. National Institute for Occupational Safety (NIOSH) and Health 8-h time-weighted average guideline at $50,000 \text{ ng m}^{-3}$ (Fig. 4). It should be noted that the interstitial air GEM measurements are potential concentrations that people may be exposed to as an acute exposure event when a disruption of the encompassing matrix occurs. The maximum GEM concentrations in the interstitial air of reprocessed mineral wastes, sediment, and soil are often observed at depth (Table S1), implying that the population is not readily exposed to these high GEM concentrations without matrix disturbance. However, the wastes may slowly emit GEM by diffusion over time. Disturbance events, such as heavy rainfall, floods, or construction activities, may initiate GEM releases of higher concentration, thereby increasing the potential for exposure as wastes retaining high concentrations of GEM are consistently dispersed throughout the urban area of Guanajuato in high traffic areas, including the university campus, residential areas, and downtown (e.g., Plaza Ranas). It is estimated that between 3000 and 5000 local inhabitants pass through Plaza Ranas daily. Additional information on potential human exposure risk is provided in Table S2. A recent study from another Ag refining region (Cedral, Mexico) attributed inhalation as the most significant exposure route of Hg to the local human population (Morton Bermea et al., 2021).

Therefore, long-term Hg monitoring of Hg in the air and human health studies (e.g., measuring Hg in hair, blood, or urine as exposure biomarkers) are recommended in the Guanajuato region to assess the potential health impact on local residents who may have been chronically exposed to Hg

and to determine whether and which mitigation measures are required. Similar studies should also be considered for other historical Ag mining regions that employed the patio process. For example, elevated Hg concentrations have been reported in the soil and river sediment in the vicinity of former *haciendas* in Cedral of Mexico (Leura Vicencio et al., 2017; Morton-Bermea et al., 2015), Potosí of Bolivia (Hagan et al., 2011; Higuera et al., 2012; Hudson-Edwards et al., 2001) and Puno of Peru (Kennedy and Kelloway, 2020).

Results from this study revealed that much of the Hg used in historical Ag refining in Hispanic America likely persists in the local environment to the present day, centuries after the use of Hg for Ag refining, in the form of calomel and its disproportionation products, GEM and Hg^{II}. This suggests that instantaneous GEM releases to the atmosphere during the patio process were much less than those from amalgamation-based Au refining processes that did not involve the formation of calomel. Despite a much lower emission factor during the patio process, the cumulative GEM emissions to the atmosphere from the disproportionation of calomel over centuries are potentially substantial, and may have an effect on the health of local residents for generations. Further studies are needed to determine the amount of calomel formed during the patio process and its disproportionation kinetics in the environment to better quantify both the instantaneous and cumulative releases of Hg to local soil, waterways, and the local and global atmosphere. This could result in major changes to global anthropogenic Hg emission inventories and affect the effectiveness of Hg emission controls prescribed in the Minamata Convention.

Funding sources

This work was financially supported by the Natural Sciences and Engineering Research Council of Canada and the Canada Research Chairs Program (F.W.), and a graduate student fellowship from the University of Manitoba (A.L., 2019).

CRediT authorship contribution statement

Ainsleigh Loria: Methodology, Investigation, Formal analysis, Data curation, Visualization, Writing – original draft. **Yann Rene Ramos-Arroyo:** Methodology, Investigation, Writing – review & editing. **Diana Rocha:** Investigation. **Gustavo Cruz-Jiménez:** Investigation. **Israel Razo Soto:** Investigation, Writing – review & editing. **Ma. Catalina Alfaro de la Torre:** Investigation, Writing – review & editing. **Debbie Armstrong:** Validation. **Saúl Guerrero:** Conceptualization, Writing – review & editing. **Feiyue Wang:** Conceptualization, Funding acquisition, Methodology, Validation, Formal analysis, Writing – review & editing.

Declaration of competing interest

The authors declare that they have no known competing financial interests or personal relationships that could have appeared to influence the work reported in this paper.

Acknowledgement

We thank Diego Díaz Barriga, José Carlos Zárate Valdovinos, José Adolfo Chávez García, Fátima Nicasio Gutiérrez, María Yanelly Zavala Guzman, Daniel Ramos-Matehuala, and Xebastian Ramos-Alvarez for volunteering their time, efforts, and enthusiasm in the field. We are grateful to Associate Editor Dr. Mae Sexauer Gustin and three anonymous reviewers for their comments and suggestions on an earlier draft of the manuscript.

Appendix A. Supplementary data

Texts S1 and S2 showing details about the GMD and the analytical method for HgI, respectively; Fig. S1 showing geographical, geological and hydrological settings of the GMD; Fig. S2 showing spatial distribution of maximum GEM concentrations in the interstitial air of reprocessed

mineral wastes, sediment, and soil across the GMD; Tables S1–S3 showing details of the study sites including potential human exposure risk, concentrations of GEM in the ground-level air and interstitial air, and total Hg concentrations and the occurrence of Hg^I in mineral waste, soil and sediment samples, respectively. Supplementary data to this article can be found online at doi:10.1016/j.scitotenv.2022.157093

References

- AMAP/UNEP, 2019. Technical Background Report for the Global Mercury Assessment 2018. Arctic Monitoring and Assessment Programme, Oslo, Norway/UN Environment Programme, Chemicals and Health Branch, Geneva, Switzerland, p. 426.
- Amos, H.M., Jacob, D.J., Streets, D.G., Sunderland, E.M., 2013. Legacy impacts of all-time anthropogenic emissions on the global mercury cycle. *Glob. Biogeochem. Cycles* 27, 410–421.
- Barnett, M.O., Harris, L.A., Turner, R.R., Stevenson, R.J., Henson, T.J., Melton, T.C., et al., 1997. Formation of mercuric sulfide in soil. *Environ. Sci. Technol.* 31, 3037–3043.
- Bayer, F.M., 2013. Quecksilberspeziation von Bergbaurückständen aus Fresnillo und Cedral, Mexiko. 2013. KarlsruheInstitute of Technology MSc. Dissertation.
- Camargo, J.A., 2002. Contribution of Spanish-American silver mines (1570–1820) to the present high mercury concentrations in the global environment: a review. *Chemosphere* 48, 51–57.
- Engstrom, D.R., Fitzgerald, W.F., Cooke, C.A., Lamborg, C.H., Drevnick, P.E., Swain, E.B., et al., 2014. Atmospheric Hg emissions from preindustrial gold and silver extraction in the Americas: a reevaluation from lake-sediment archives. *Environ. Sci. Technol.* 48, 6533–6543.
- Guerrero, S., 2012. Chemistry as a tool for historical research: identifying paths of historical mercury pollution in the Hispanic New World. *Bull. Hist. Chem.* 37, 61–70.
- Guerrero, S., 2016. The history of silver refining in New Spain, 16C to 18C: back to basics. *Hist. Technol.* 32, 2–32.
- Guerrero, S., 2017. Silver by Fire, Silver by Mercury: A Chemical History of Silver Refining in New Spain and Mexico, 16th to 19th Centuries. Brill, Leiden, the Netherlands.
- Guerrero, S., 2018. The environmental history of silver production, and its impact on the United Nations Minamata Convention on mercury. Extended Abstract, Session on Global Production and Distribution of Silver, World Economic History Congress, Boston, USA, July 29 - August 3, 2018. Available at: <http://wehc2018.org/wp-content/uploads/2018/04/WEHCguerreroMinamata2.pdf>.
- Gustin, M.S., Biester, H., Kim, C.S., 2002. Investigation of light enhanced emission of mercury from naturally enriched substrate. *Atmos. Environ.* 36, 3241–3254.
- Hagan, N., Robins, N., Hsu-Kim, H., Halabi, S., Morris, M., Woodall, G., et al., 2011. Estimating historical atmospheric mercury concentrations from silver mining and their legacies in present-day surface soil in Potosí, Bolivia. *Atmos. Environ.* 45, 7619–7626.
- Higuera, P., Llanos, W., García, M.E., Millán, R., Serrano, C., 2012. Mercury vapor emissions from the Ingenios in Potosí (Bolivia). *J. Geochem. Explor.* 116, 1–7.
- Hudson-Edwards, K.A., Macklin, M.G., Miller, J.R., Lechler, P.J., 2001. Sources, distribution and storage of heavy metals in the Río Pilcomayo, Bolivia. *J. Geochem. Explor.* 72, 229–250.
- Johnson, D.A., Whittle, K., 1999. The chemistry of the Hispanic-American amalgamation process. *Dalton Trans.* 4239–4243.
- Kennedy, S.A., Kelloway, S.J., 2020. Identifying metallurgical practices at a colonial silver refinery in Puno, Peru, using portable X-ray fluorescence spectroscopy (pXRF). *J. Archaeol. Sci. Rep.* 33, 102568.
- Kim, C.S., Rytuba, J.J., Brown, G.E., 2004. Geological and anthropogenic factors influencing mercury speciation in mine wastes: an EXAFS spectroscopy study. *Appl. Geochem.* 19, 379–393.
- Lacerda, L.D., Salomons, W., 1999. Mercury contamination from the New World gold and silver mine tailings. In: Ebinghaus, R., Turner, R., Lacerda, L.D., Vasiliev, O., Salomons, W. (Eds.), *Mercury Contaminated Sites: Characterization, Risk Assessment and Remediation*. Springer, Heidelberg, pp. 73–87.
- Leura Vicencio, A.K., Carrizales Yañez, L., Razo, Soto I., 2017. Mercury pollution assessment of mining wastes and soils from former silver amalgamation area in North-Central Mexico. *Rev. Int. Contam. Ambient.* 33, 655–669.
- Lumex Instruments, RA-915M: direct determination of mercury content in ambient air. <https://www.lumexinstruments.com/metodics/16AE08.01.01-1.pdf>.
- Morton Bermea, O., Castro-Larragoitia, J., Arellano Álvarez, Á.A., Pérez-Rodríguez, R.J., Leura-Vicencio, A., Schiavo, B., et al., 2021. Mercury in blood of children exposed to historical residues from metallurgical activity. *Expo. Health* 13, 281–292.
- Morton-Bermea, O., Jiménez-Galicia, R.G., Castro-Larragoitia, J., Hernández-Álvarez, E., Pérez-Rodríguez, R., García-Arreola, M.E., et al., 2015. Anthropogenic impact of the use of Hg in mining activities in Cedral S.L.P. Mexico. *Environ. Earth Sci.* 74, 1161–1168.
- Nriagu, J.O., 1993. Legacy of mercury pollution. *Nature* 363, 589.
- Nriagu, J.O., 1994. Mercury pollution from the past mining of gold and silver in the Americas. *Sci. Total Environ.* 149, 167–181.
- Outridge, P., Mason, R., Wang, F., Guerrero, S., Heimburger-Boavida, L.-E., 2018. Updated global and oceanic mercury budgets for the United Nations Global Mercury Assessment 2018. *Environ. Sci. Technol.* 52, 11466–11477.
- Ramos-Arroyo, Y.R., Prol-Ledesma, R.M., Siebe-Grabach, C., 2004. Características geológicas y mineralógicas e historia de extracción del distrito de Guanajuato, México. *Rev. Mex. Cienc. Geol.* 21, 268–284.
- Randall-Roberts, J.A., Saldaña, E., Clark, K.F., 1994. Exploration in a volcano-plutonic center at Guanajuato, México. *Econ. Geol.* 89, 1722–1751.
- Robins, N.A., Hagan, N., Halabi, S., Hsu-Kim, H., Dario, R., Gonzales, E., et al., 2012. Estimations of historical atmospheric mercury concentrations from mercury refining and present-day soil concentrations of total mercury in Huancavelica, Peru. *Sci. Total Environ.* 426, 146–154.

- Schlüter, K., 2000. Review: evaporation of mercury from soils. An integration and synthesis of current knowledge. *Environ. Geol.* 39, 249–271.
- Sholupov, S., Pogarev, S., Ryzhov, V., Mashyanov, N., Stroganov, A., 2004. Zeeman atomic absorption spectrometer RA-915+ for direct determination of mercury in air and complex matrix samples. *Fuel Process. Technol.* 85, 473–485.
- Sillitoe, R., 2009. Supergene silver enrichment reassessed. In: Titley, S.R. (Ed.), *Supergene Environments, Processes and Products*. 14. Society of Economic Geologists, Spec. Pub, pp. 15–32.
- Streets, D.G., Devane, M.K., Lu, Z., Bond, T.C., Sunderland, E.M., Jacob, D.J., 2011. All-time releases of mercury to the atmosphere from human activities. *Environ. Sci. Technol.* 45, 10485–10491.
- Streets, D.G., Horowitz, H.M., Jacob, D.J., Lu, Z., Levin, L., ter Schure, A.F.H., et al., 2017. Total mercury released to the environment by human activities. *Environ. Sci. Technol.* 51, 5969–5977.
- Streets, D.G., Horowitz, H.M., Lu, Z., Levin, L., Thackray, C.P., Sunderland, E.M., 2019. Five hundred years of anthropogenic mercury: spatial and temporal release profiles. *Environ. Res. Lett.* 14, 084004.
- Svensson, M., Allard, B., Düker, A., 2006. Formation of HgS – mixing HgO or elemental Hg with S, FeS or FeS₂. *Sci. Total Environ.* 368, 418–423.
- U.S. EPA, 2007. Method 7473 (SW-846): Mercury in Solids and Solutions by Thermal Decomposition, Amalgamation, and Atomic Absorption Spectrophotometry. United States Environmental Protection Agency, Washington, DC.
- Wang, Y., Liu, G.L., Li, Y.B., Liu, Y.W., Guo, Y.Y., Shi, J.B., et al., 2020. Occurrence of mercurous [Hg(I)] species in environmental solid matrices as probed by mild 2-mercaptoethanol extraction and HPLC-ICP-MS analysis. *Environ. Sci. Technol. Lett.* 7, 482–488.
- Zhang, Y., Jaeglé, L., Thompson, L., Streets, D.G., 2014. Six centuries of changing oceanic mercury. *Glob. Biogeochem. Cycles* 28, 1251–1261.